J Comp Physiol A (1998) 182: 89–101 © Springer-Verlag 1998

ORIGINAL PAPER

T. C. Tricas · J. G. New

Sensitivity and response dynamics of elasmobranch electrosensory primary afferent neurons to near threshold fields

Accepted: 20 June 1997

Abstract Elasmobranch fishes localize weak electric sources at field intensities of <5 ηV cm^{-1}, but the response dynamics of electrosensory primary afferent neurons to near threshold stimuli in situ are not well characterized. Electrosensory primary afferents in the round stingray, *Urolophus halleri*, have a relatively high discharge rate, a regular discharge pattern and entrain to 1-Hz sinusoidal peak electric field gradients of ≤20 ηV cm^{-1}. Peak neural discharge for units increases as a non-linear function of stimulus intensity, and unit sensitivity (gain) decreases as stimulus intensity increases. Average peak rate-intensity encoding is commonly lost when peak spike rate approximately doubles that of resting, and for many units occurs at intensities <1 μV cm^{-1}. Best neural sensitivity for nearly all units is at 1–2 Hz with a low-frequency slope of 8 dB/decade and a high-frequency slope of −23 dB/decade. The response characteristics of stingray electrosensory primary afferents indicate sensory adaptations for detection of extremely weak phasic fields near 1–2 Hz. We argue that these properties reflect evolutionary adaptations in elasmobranch fishes to enhance detection of prey, communication and social interactions, and possibly electric-mediated geomagnetic orientation.

Key words Electroreception · Elasmobranch · Neural sensitivity · Response dynamics · Sensory biology

Abbreviations *AEN* ascending efferent neuron · *CV* coefficient of variation · *DC* resting discharge · *EOD* electric organ discharge · *PTP* peak-to-peak

T.C. Tricas (✉)
Department of Biological Sciences,
Florida Institute of Technology, 150 West University Boulevard,
Melbourne, FL 32901-6988, USA,
Fax.: +1-407 952-1818; e-mail: tricas@fit.edu

J.G. New
Department of Biology and Parmly Hearing Institute,
6525 N. Sheridan Road, Loyola University, Chicago,
IL 60626, USA

Introduction

Ampullary electroreceptors form an elaborate sensory system in most living non-teleost fishes, some osteoglossomorph and ostariophysan teleosts, and many aquatic amphibians. In the Elasmobranchii (rays, skates and sharks) the ampullae of Lorenzini are grouped into several subdermal cephalic clusters from which project radial canals that terminate at pores on the skin. This system samples weak extrinsic voltage gradients that occur across the body and encodes information about the direction, polarity, and intensity of the source (review: Bodznick and Boord 1986).

The biological role of electroreception in elasmobranchs is known to include the location of weak direct current (d.c.) fields produced by prey (Kalmijn 1971; Tricas 1982) and is theorized to be important for orientation and navigation behavior via geomagnetic induction (Murray 1962; Kalmijn 1974; Paulin 1995). Recent work on the round stingray (*Urolophus halleri*) has expanded electrosensory function to include social behaviors such as the detection and localization of conspecifics during mating activity in wild populations (Tricas et al. 1995). Both male and female stingrays detect weak bioelectric fields produced by visually cryptic females that are buried in the sand. These weak bioelectric stimuli arise from ionic charges at skin and buccal membranes in contact with the water and are modulated by ventilatory movements of the spiracles, gill slits, and mouth (Kalmijn 1974; Bodznick et al., 1992). Round stingrays show behavioral responses to uniform electric fields of 5 ηV cm^{-1} (Kalmijn 1982) and their electrosensory primary afferent neurons can encode the modulation of extrinsic ventilatory fields produced by conspecifics (Tricas et al. 1995).

Whereas both extrinsic and self-generated ventilatory potentials are known to modulate the resting discharge of primary afferent neurons (Dijkgraaf and Kalmijn 1966; Akoev et al. 1976; Montgomery 1984a) only a few physiological studies have attempted to characterize

their intensity and frequency responses. Murray (1962, 1965) first established the sensitivity of the receptor system for a reduced in situ preparation in the skate (*Raja ocellata*) by recording primary afferent responses to brief pulsed current applied at the canal pore, and showed an approximately linear stimulus intensity-response relationship at currents up to about 6 ηA. Later workers characterized the low-frequency response of batoid primary afferent neurons between 0.1 and 10 Hz (e.g. Andrianov et al. 1983; Montgomery 1984b; New 1990). However, dissimilar experimental methodologies have precluded rigorous species comparisons of sensitivity thresholds, tuning peaks and frequency roll-offs, and the linearity of the stimulus intensity-response relationships for electrosensory primary afferents. This is further confounded by the use of stimuli orders of magnitude above the <1 μV cm^{-1} field threshold for primary afferents reported by Murray (1962) and Andrianov et al. (1984), and therefore frequency responses may be characterized in non linear regions or at higher intensities where neural responses are saturated. Examination of neural response dynamics near threshold is especially relevant since electric orientation behaviors in free-swimming elasmobranchs are known to be evoked at field intensities as low as 5 ηV cm^{-1} (Kalmijn 1982). The stimulus-response relationships and associated frequency tuning curves to these near-threshold and biologically important intensities must be characterized to understand how natural electrosensory information is processed centrally.

This study characterizes the response properties of electrosensory primary afferent neurons in *Urolophus* to weak near-threshold fields which are known to be important cues in their natural social and orientation behaviors. Our experiments on *Urolophus* show that primary afferents can encode peak electric field gradients of ≤20 ηV cm^{-1}, are tuned at 1–2 Hz, and have a nonlinear stimulus-response function that can saturate at intensities well below 1 μV cm^{-1}. We interpret these findings in terms of electrosensory adaptations that maximize the probability of detection of mates, prey and other biologically important electric sources in their natural environment.

Materials and methods

Preparation and neurophysiology

Adult round stingrays (*U. halleri*) of 20–30 cm disk width were collected in coastal waters of southern California, shipped to the Florida Institute of Technology and maintained in a refrigerated aquarium at 18 °C. Experimental fish were lightly anesthetized by immersion in a seawater bath containing 0.025% tricaine methanesulfonate and immobilized by an intramuscular injection of pancuronium bromide (0.3 mg kg^{-1} body weight) sufficient to suppress muscular control of ventilatory activity. The hyomandibular cranial nerve, which carries primary afferent fibers from the hyoid and mandibular clusters of ampullae of Lorenzini, was surgically exposed above the waterline immediately caudal to the left spiracular opening. Animals were mounted on a horizontal stage in a 61 cm long × 41 cm wide × 15 cm deep acrylic experimental tank supplied with electrically isolated refrigerated seawater at 18 °C and a resistivity of 20–22 Ω cm^{-1} (Fig. 1). Fish were ventilated by a continuous flow of fresh seawater into the mouth and across the epibranchial chambers.

Extracellular recordings were made with glass microelectrodes (4 mol·l^{-1} NaCl, 7–20 MΩ) visually guided to the surface of the nerve. Electrosensory primary afferent units were identified by their response to a 2- to 4-μV cm^{-1}, 1-Hz sinusoid bipolar uniform search stimulus delivered to the tank. Prior to stimulation experiments 500 consecutive spikes were collected for each neuron for determination of resting discharge (DC) rate and regularity. Analog unit discharges were amplified, filtered at 300–3 kHz, and the analog signals stored on tape for later analyses.

Weak bioelectric fields encountered in the wild are composed of both standing and modulated d.c. field components (Kalmijn 1974; Tricas et al. 1995). Electroreceptors were stimulated using either a sinusoidal or pulsed electric field that was generated by an arbitrary function generator and an isolation amplifier. Stimulus current was delivered to the experimental tank via sets of carbon electrodes spaced 40 cm apart and aligned on the rostral-caudal (longitudinal) and transverse axes of the fish's disk (Fig. 1). Care was taken to minimize any standing d.c. junction potentials that might be generated by the carbon electrodes. Electrode pairs were initially conditioned by coupling their input terminals while they soaked in seawater over many days. After preparation the experimental animals were allowed to acclimate undisturbed in the experimental apparatus for at least 0.5 h before recordings began and is sufficient time to permit full accommodation of the electrosensory system to any d.c. fields (Bodznick et al. 1993). No extraneous fields were detected in the experimental tank with our differential amplifier monitor, and lifting the electrodes from the tank (eliminating a possible standing field) had no effect on the DC rate of primary afferent neurons.

Frequency response curves were determined for 0.01- to 30-Hz stimuli. A sinusoidal bipolar burst of constant peak amplitude was delivered across the body along the more sensitive of the two axes. For each stimulus frequency a minimum of 500 spikes were collected over at least one cycle of stimulation. The analog stimulus signal, analog unit data and digital synch pulse mark were recorded during all experiments. DCs were routinely sampled between frequency stimulations to verify a consistent discharge for each afferent over the course of the 15- to 20-min experiment. Additional frequency response information was obtained by recording discharge response to a pulsed constant current field.

Stimulus intensities were measured by differential recording with Ag-AgCl electrodes positioned along the stimulus axes. Bipolar sinusoidal stimulus voltages were measured peak-to-peak (PTP) and then converted to peak (1/2 PTP). Prior to stimulation, any d.c. offset present at the output of the stimulus isolation amplifier was nulled. Routine stimulus field intensities used for linear response dynamics experiments ranged from 0.04 to 2.0 μV cm^{-1} PTP. For determination of frequency-tuning curves, sinusoidal stimuli were chosen so that the peak discharge was 25–75% above DC rate when stimulated at 1 Hz. Careful effort was made in these experiments to avoid full (100%) modulation of unit resting activity because of the associated saturation response (see Results).

Data analyses

All analyses were conducted off-line. Discriminated analog unit discharges, stimulus waveforms, and stimulus synch pulses from tape were converted to digital computer files via a Cambridge Electronic Design 1401 running under Spike 2 software. DCs were characterized from 500 consecutive spikes and used to generate an interspike interval histogram. Discharge regularity was expressed as the coefficient of variation (CV), a dimensionless ratio of standard deviation to mean interspike interval. Interspike interval histogram distributions were analyzed for skewness (an indicator of distribution symmetry) and kurtosis (an indicator of peak shape) using the moment statistics g_1 and g_2, respectively, to assess

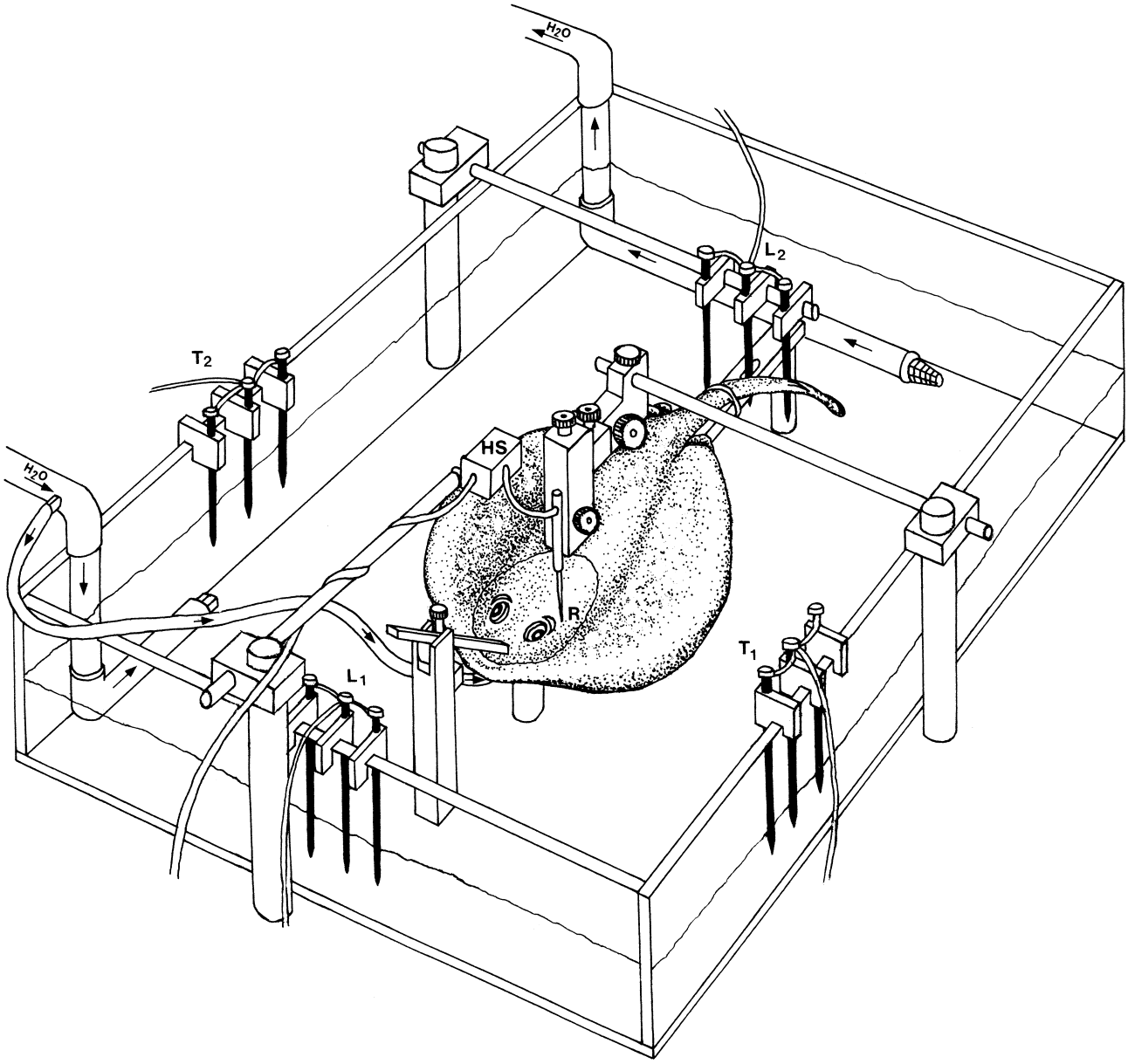

Fig. 1 Experimental apparatus used for recording discharges of electrosensory primary afferents in the round stingray, *Urolophus halleri*. The immobilized fish was clamped in an acrylic tank (61 cm long × 41 cm wide × 15 cm deep) filled with seawater to a level just below the eye and ventilated through the mouth (*arrows*). A small dorsal incision was made behind the spiracle to expose the hyomandibular nerve, the recording electrode (*R*) lowered, and unit discharges preamplified via a head stage (*HS*). Stimulus fields were delivered across the disk via sets of carbon electrodes positioned along the transverse (T_1 and T_2) and longitudinal (L_1 and L_2) axes of the body

discharge patterns relative to that predicted by a normal distribution (Sokal and Rohlf 1981). The stimulus response of electrosensory units to sinusoidal stimulation was calculated by determining the relationship of peak discharge rate as a function of peak stimulus intensity across 1-Hz test frequency. Linearity of the relationship was tested by least-squares regression analysis.

Period histograms were constructed for evaluation of neural sensitivity and phase response across stimulus frequencies. At least 500 consecutive spikes were collected for at least one stimulus cycle and displayed in a period histogram divided into 128 bins. A Fourier transformation was performed on the period histogram to generate coefficients for mean firing rate (DC), peak discharge rate, and phase relationship of the unit response to the stimulus. With these parameters a sinusoid curve was fit to the empirical data. The DC firing rate calculated by this method at near-threshold stimulus intensities was indistinguishable from the actual mean resting rate of 20 neurons (paired *t*-test, $t = 2.09$, $df = 19$, $P = 0.83$). This demonstrates that units are symmetrically modulated about the resting rate by near-threshold excitatory cathodal and inhibitory anodal stimuli, and that primary afferents exhibit no major shift in DC firing rate associated with stimulus amplitude within this response range; however, see linear response analysis of DC shift at higher stimulus intensities in Results.

The maximum neural response to a uniform electric field in the experimental tank occurs when the field is parallel to the main axis of the canal, and decreases as a cosine function of the angle of deviation. For canals not aligned with either major axis of stimulation, peak discharge for a parallel field was estimated by the following method. First, peak unit responses were recorded for

fields applied along the transverse and longitudinal axes. Next, the angular deviation of the canal from the transverse axis was estimated by the arctangent of their gain (peak-DC) ratio. Finally, neural gain to a field applied parallel to the canal was estimated by the product of the measured gain along one axis and the associated secant (transverse axis) or cosecant (longitudinal axis) identity. Percent modulation of the DC rate was expressed as [(peak-DC)/DC] × 100. Neural sensitivity was expressed as the increase in peak spike rate above DC (peak minus DC discharge rate) per one-half the PTP stimulation intensity, or spikes s^{-1} μV^{-1} cm^{-1}. The phase relation between stimulus and neural discharge response was expressed as the difference in arc degrees between the peak discharge rate and peak stimulus amplitude.

Results

Resting discharge patterns of electrosensory primary afferent neurons

DC activity in the absence of exogenously applied electrical stimulation was recorded from a total of 80 primary afferent electrosensory neurons in 19 sexually mature stingrays. DC rates ranged from 22.2 to 41.7 spikes s^{-1} (34.2 ± 5.0; $\bar{x} \pm$ SD). The vast majority of primary afferent electrosensory neurons in healthy fish showed a discharge pattern of regularly spaced interspike intervals without interruption in the discharges as seen in Figure 2A; however, interspike interval duration was not distributed randomly about the mean. Figure 3 shows the recorded interspike interval histograms and the normal distribution for three representative afferents with resting discharge rates near the population mean. Histograms for units with a low CV (e.g., Fig. 3, top) were bilaterally symmetrical ($g_1 = 0.08 \pm 0.21$; ± 95% confidence limits, CL), leptokurtotic ($g_2 = 0.92 \pm 0.43$) but rarely encountered. In comparison, units with an intermediate CV (e.g. Fig. 3, middle) were typically skewed slightly to the right ($g_1 = 0.71 \pm 0.21$) and leptokurtotic ($g_2 = 1.70 \pm 0.43$). Units with the highest CVs (Fig. 3, bottom) were similar to intermediate CV units ($g_1 = 0.71 \pm 0.22$; $g_2 = 1.09 \pm 0.43$). The leptokurtotic distribution common to most units indicates that discharges are concentrated more near the mean than would be expected in a normal distribution and indicates a high degree of endogenous discharge regularity.

The discharge variability is reflected in CV values that ranged from 0.13 to 0.34 (0.22 ± 0.04; $\bar{x} \pm$ SD). When the DC rates of all units are considered, a negative but weak association was identified between interspike interval and CV (Fig. 4). The CV of primary afferent vestibular units is known to vary as a function of mean discharge rate, but we did not attempt a comparison among units in which the mean resting interval was standardized (see Goldberg et al. 1984). Rather we modeled a linear relationship for these discharge characteristics (H_o: $\beta = 0$, $t = 2.58$, $P < 0.012$) but little of the discharge variability was explained by the mean resting interspike interval of the unit ($r^2 = 0.08$) because of the high variability among units.

Fig. 2A–C Resting and evoked discharge patterns of primary afferent neurons in the electrosensory system of the immobilized round stingray, *U. halleri*. **A** Extracellular recording of DC over a period of 4 s. Note that interspike intervals are spaced relatively evenly. **B** Modulation of discharge pattern by a uniform electric field applied across the body. *Top trace* shows the 1-Hz bipolar stimulus. *Bottom five traces* show discharges of the unit in relation to increasing peak stimulus intensity which is indicated on left. The DC is modulated by cathodal (excitatory) and anodal (inhibitory) stimuli as a function of stimulus intensity. Full (100%) modulation for this unit occurred at a peak stimulus intensity of about 0.13 μV cm^{-1}. Graphs at right show the associated period histograms to which sinusoidal curves were fit and used to determine intensity and frequency responses. **C** DC pattern of an oscillating-type electrosensory primary afferent. One cycle of discharge has a rapid onset, lasts for 1–2 s and is followed by a silent period of about 3–4 s. These units were rarely encountered, relatively unresponsive to electric field stimulation and therefore were not used in the intensity or frequency response experiments. Bar = 5 s. ►

While regularly spaced interspike intervals were clearly the predominant discharge pattern among individuals of this species, in 4 of 19 fish (21%) most primary afferent DCs occurred in rapid bursts separated by silent periods lasting a few seconds (Fig. 2C) similar to that reported for *Scyliorhinus* (Braun et al. 1994). However, these units typically required up to ten times the stimulus intensity used to modulate units with the regular DC pattern. Furthermore, for the few fish in which these two classes of units did co-occur, we qualitatively observed that the proportion of bursting fibers encountered increased over the course of the 6- to 24-h experiments. We therefore considered the bursting of spikes by electrosensory primary afferents to be an anomalous physiological condition and therefore we did not conduct a response analysis on those units.

Response to electrosensory stimuli

Stimulation of electroreceptors with a sinusoidal electric field modulates the neural discharge as a function of stimulus intensity. Figure 2B shows the discharge pattern of a representative electrosensory unit to a bipolar sinusoid stimulus delivered at 1 Hz and also their associated period histograms. At low stimulus amplitudes the regular DC is modulated by the bipolar cathodal (excitatory) and anodal (inhibitory) stimulus phases. Note that the peak discharge is in phase with the cathodal stimulus peak, the minimum discharge in phase with the anodal peak, and that the modulation encodes the stimulus waveform (Fig. 2B; trace 2, 3). As stimulus intensity increases so does percent modulation of the unit until peak discharge doubles that of resting. At higher stimulus intensities, unit discharges are clipped at the anodal peak (Fig. 2B; trace 5, 6) and in many units the averaged amplitude of the discharge also saturates (Fig. 5A; B). In this case, the average peak discharge does not increase but rather decreases with increasing stimulus intensity. However, the peak discharge continues to be phase locked to the stimulus. Thus, when primary afferents are less than fully modulated both

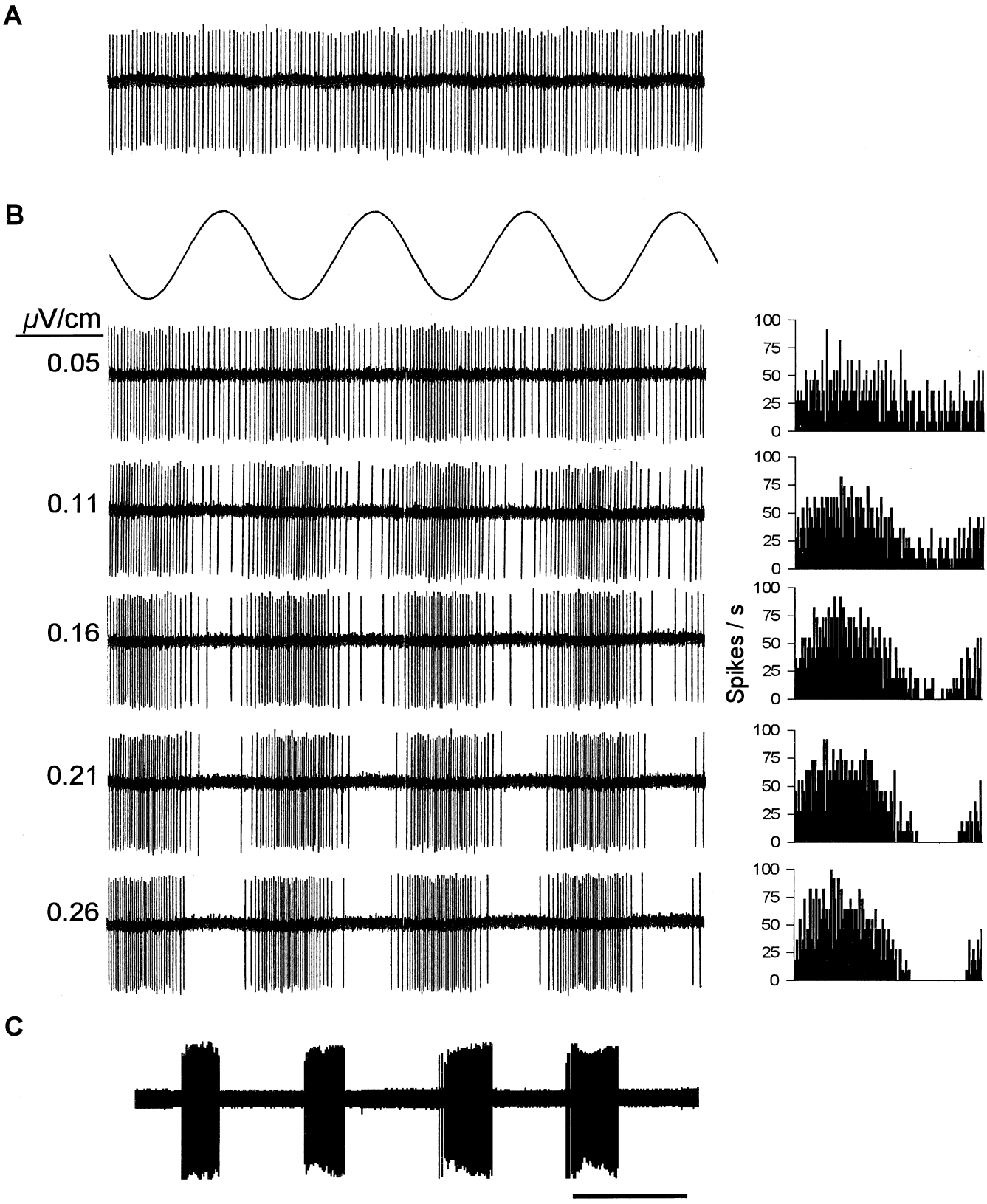

intensity and temporal information are encoded by primary afferents, but only temporal information is reliably encoded when the unit discharge is clipped.

Stimulus thresholds, rate-intensity response and linearity

Response thresholds were defined for electrosensory afferents as the lowest applied intensity at which peak

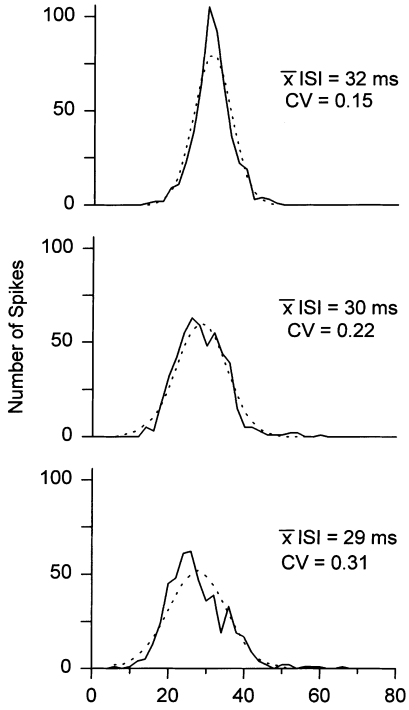

Fig. 3 Regularity of discharge among electrosensory primary afferent neurons in the round stingray, *U. halleri*. Interspike interval (*ISI*) distributions are shown for three primary afferent units (*solid line*) with DC rates near the mean ISI of all units ($x = 29$ ms, $n = 81$). Most distributions were strongly leptokurtotic due largely to occasional intervals that were two to three times longer than the mean. For a given average DC rate among different fibers, there exists a four fold difference in their ISI variances. Theoretical normal distributions with the same mean and standard deviation are indicated by *dashed lines*

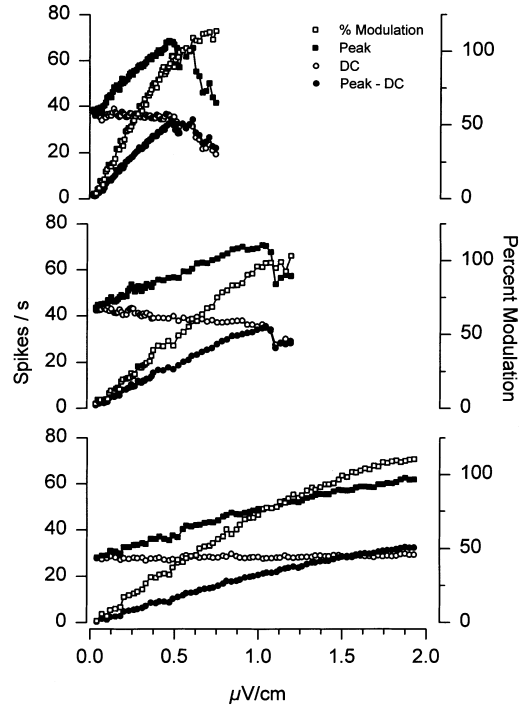

Fig. 5 Relationship between stimulus intensity and response of three representative electrosensory primary afferents in *U. halleri*. *Top graph* shows that neural discharge (seen in the peak and peak-DC curves) for the high gain unit increases as a function of stimulus intensity but this relationship is lost when the unit is fully modulated at intensities near 0.5 μV cm^{-1}. *Middle plot* shows the response for an intermediate gain unit that saturates at intensities above 1 μV cm^{-1}. Units with low gain characteristics (*bottom plot*) have a lower sensitivity but encode across a wider range of stimulus intensities. Note also that mean DC discharge level decreases slightly for the more sensitive units as stimulus intensity is increased. Amplitude on *abscissa* is peak-to-peak

phase remained aligned with that of suprathreshold stimuli (near 0 ° re: cathodal phase of a 1-Hz bipolar stimulus). Voltage field thresholds measured for primary afferents ranged from 40 ηV cm^{-1} PTP (= 20 ηV cm^{-1}

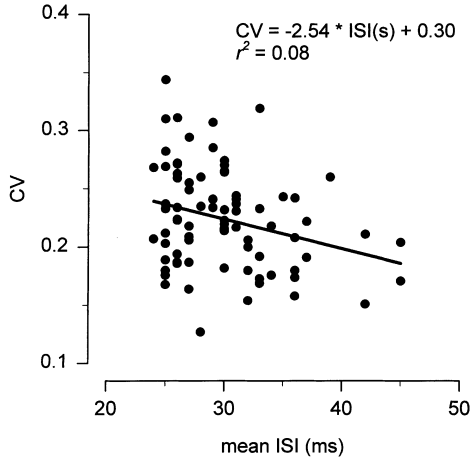

Fig. 4 Relationship between discharge regularity and ISI for electrosensory primary afferent neurons in *U. halleri*. Slower discharging units have a greater regularity (lower CV) but the biological significance of the relationship is doubtful because of the high variability for a given discharge rate

peak) to several μV cm^{-1} PTP. Intensity sweeps performed on the most sensitive units encountered showed measurable modulation of resting discharge at a mean intensity of 40 ± 20 (SD) ηV cm^{-1} PTP ($n = 9$). The peak modulation calculated for these units to the low intensity stimulus was usually within 5° of the peak of the stimulus, and provides confirmation of phase alignment of the neural response with the stimulus (see phase relation at best frequency below). A measurable modulation to a 40-ηV cm^{-1} PTP field was found for seven hyoid units which is equivalent to a 20 ηV cm^{-1} peak stimulus. However, it is likely that many neurons could be modulated at even lower intensities.

All recorded units showed an increase in peak discharge to increased intensity of electrical stimulation. Among fibers for which gain was calculated at 1 Hz, neural sensitivity ranged widely from 1.7 to 80.3 spikes s^{-1} μV^{-1} cm^{-1} with a mean of 24.3 ± 20.6 (SD) spikes s^{-1} μV^{-1} cm^{-1} ($n = 14$). The relationship between unit discharge and stimulus intensity is shown in Fig. 5 for three representative afferent fibers recorded from a single ray. At stimulus intensities that modulate the DC below 100%, the peak neural discharge for all fibers is an increasing function of stimulus intensity. In the

example shown, the most sensitive primary afferent (Fig. 5, top) had a more than threefold greater average peak discharge slope across the full stimulus intensity range compared to the unit with the lowest sensitivity (Fig. 5, bottom). The broad range of sensitivities recorded for units is undoubtedly due at least partially to differences in canal length among fibers, but also partly due to non-linearity in the stimulus-response relationship described below.

The average DC firing rate during stimulation computed for low sensitivity units showed little change across the range of stimulus intensities. For example, the mean firing rate of the low-gain unit shown in Table 1 increased by only 0.71 spikes s^{-1} for each 1 μV cm^{-1} increase in stimulus intensity. However, for the units with a more robust response to sinusoidal bipolar stimuli, DC discharge rate was an inverse function of peak stimulus intensity as shown by the negative slope (β) and the decrease of as much as 10–20% across the full stimulus range. When the DC firing rate is subtracted from the peak discharge the estimate of neural sensitivity (slope of peak – DC) remains an increasing function of stimulus intensity and is further enhanced in some units.

Although unit discharge rate clearly increases as a function of stimulus intensity below the 100% modulation level, neural sensitivity generally decreases with increased stimulus intensity. A sequential segment analysis of gain across the full range of modulation in the example fibers described above shows a distinct change in the rate-intensity response relationship (Fig. 6). For the most sensitive unit (top curve) neural gain averaged 80.3 spikes s^{-1} μV^{-1} cm^{-1} at stimulus intensities up to approximately 0.20 μV cm^{-1} but showed a rapid decline to 49.6 spikes s^{-1} μV^{-1} cm^{-1} at twice the stimulus intensity, or approximately a 38% decline in neural sensitivity. Similar decreases in neural sensitivity occur at increasing stimulus intensities for both the intermediate (middle curve, 46% decline) and low (bottom curve, 54% decline) gain example units. It appears that the instantaneous gain is a decreasing function of stimulus intensity and is most marked in high gain units. These data do not support the existence of a linear stimulus response relationship for intensity encoding by primary afferents at near and supra-threshold stimulus intensities.

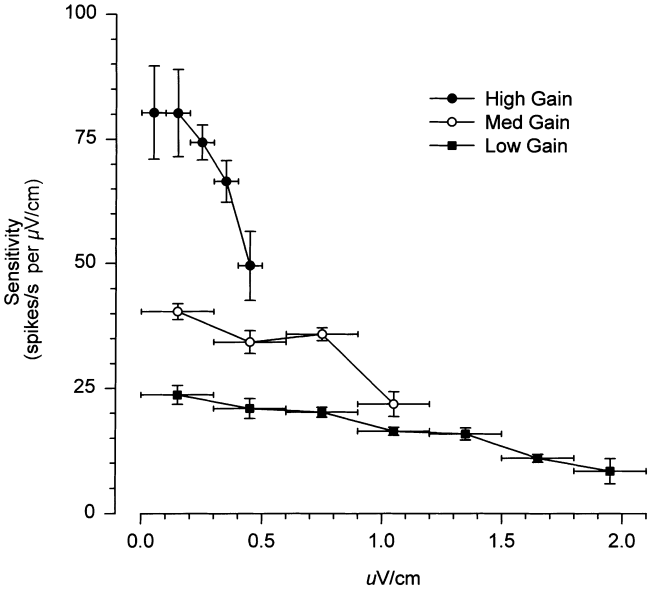

Fig. 6 Sequential linearity analysis for stimulus-response of electrosensory primary afferent units shown in Fig. 5. In this analysis the relationship between stimulus intensity and neural response (peak-DC) was calculated for 10 successive data points and their slopes plotted as a function of average stimulus intensity. Note that for the most sensitive unit (*top curve*) gain is maintained at about 80 spikes s^{-1} μV cm^{-1} only up to stimulus intensities about 0.2 μV cm^{-1}. At higher stimulus intensities sensitivity falls off sharply. Less sensitive units also show a significant but less rapid decrease in neural sensitivity as stimulus intensity is increased. *Horizontal bars* indicate range of stimulus intensity for which mean sensitivity was calculated. *Vertical bars* indicate standard error of sensitivity for each group. Amplitude on *abscissa* is peak-to-peak

The increasing stimulus response relationship deteriorates as unit discharges exceed full modulation (peak discharge rate = approximately twice that of the DC rate) and was most evident for high-gain units. For example, in the two top units in Fig. 5 there is a marked change in the curves at stimulus intensities near or < 1 μV cm^{-1} for peak-DC, and the resultant peak-DC firing rates which corresponds to the region where the units are fully modulated. As a result, the positive relationship between average peak discharge and stimulus intensity changed to an unpredictable function. In contrast, the low gain unit (Fig. 5, bottom) showed no evident saturation near the 2 μV cm^{-1} maximum stimulus

Table 1 Parameters of stimulus intensity relationships for resting discharge (DC), peak, and peak-DC neural responses in three electrosensory primary afferent neurons recorded from an adult round stingray, *Urolophus halleri*. Unit sensitivity is categorized by relative sensitivity to show range of neural responses to sinusoidal stimulation. β = slope of stimulus- response regressions ±95% confidence limit

Unit sensitivity	Resting rate (spikes s^{-1})	DC	Peak	Peak-DC
Low	27	$\beta = 0.71 \pm 0.33$ $r^2 = 0.46$	$\beta = 20.1 \pm 0.64$ $r^2 = 0.99$	$\beta = 19.38 \pm 0.47$ $r^2 = 0.99$
Medium	43	$\beta = -7.20 \pm 0.86$ $r^2 = 0.85$	$\beta = 28.08 \pm 1.04$ $r^2 = 0.98$	$\beta = 35.29 \pm 0.79$ $r^2 = 0.99$
High	37	$\beta = -3.22 \pm 1.67$ $r^2 = 0.20$	$\beta = 66.02 \pm 3.11$ $r^2 = 0.97$	$\beta = 69.24 \pm 2.13$ $r^2 = 0.99$

intensity delivered in the experiment. In general, when peak discharge of electrosensory afferents exceeds approximately twice that of a unit's DC rate, the encoding of average rate-intensity information is lost.

Intensity response as a function of stimulus frequency

The response of a representative fiber to a sinusoidal stimulus delivered across a range of intensities and frequencies is shown in Fig. 7. At stimulus intensities ≤ 0.05 μV cm^{-1} PTP the period histograms are flat and the analysis was unable to demonstrate entrainment to the stimulus by this neuron. As the bipolar stimulus intensity is increased above this level so are the maximum and minimum peak excursions from DC. Within a constant stimulus intensity that evokes less than 100% modulation, the greatest discharge peak is consistently observed for stimulus frequencies near 1–2 Hz. Note that for this unit the response is modulated fully at intensities of about 0.4 μV cm^{-1} PTP. At greater anodal stimulation the unit response is clipped and has a truncated conduction. This response to relatively intense stimuli exceeds the linear response range described above. The period histogram matrix of Fig. 7 also shows alignment of peaks for both the stimulus and neural response across stimulus intensities. At lower frequencies peak neural response shows a progressive phase lead and at higher frequencies a progressive phase lag. Thus, although intensity information encoded by primary afferents changes with stimulus intensity in a non-linear manner, the temporal relationship between the stimulus and neural response peaks is constant for each stimulus frequency.

The intensity-response relationship is maintained but attenuated at frequencies above and below 1–2 Hz. Figure 8 shows the response curves for stimuli delivered to a representative unit across almost three frequency decades. An increasing stimulus-response relationship is seen below 100% modulation of the DC rate but becomes asymptotic as the maximum discharge peak is approached. Low-frequency responses were estimated by calculation of time-constants of decay following stimulation with a series of unipolar d.c. step stimuli. Figure 9 shows the averaged decay of a representative primary afferent with a time-constant of about 4 s. A negative exponential model was fit to the d.c. step response data and time constants calculated. Observed instantaneous average peak discharge varied greatly among fibers and ranged from 22.6–70.5 spikes s^{-1} ($\bar{x} \pm \mathrm{SD} = 47.0 \pm 17.2$) above resting. However, the peak afferent discharge above resting estimated by the exponential model (range = 8.3–47.0 spikes s^{-1}, ($\bar{x} \pm \mathrm{SD} = 27.0 \pm 13.7$) typically underestimated the

Fig. 7 Period histogram response matrix for a representative electrosensory primary afferent fiber. Best frequency response for this unit is at approximately 1 Hz. At 1 Hz stimulation, the unit is weakly modulated at 0.08 μV cm^{-1}, fully modulated at about 0.4 μV cm^{-1} and is saturated at higher stimulus intensities. The electrosensory primary afferents can encode both lower- and higher-frequency information when stimulated at higher intensities. Stimulus frequency increases from left to right, and peak-to-peak intensity increases top to bottom

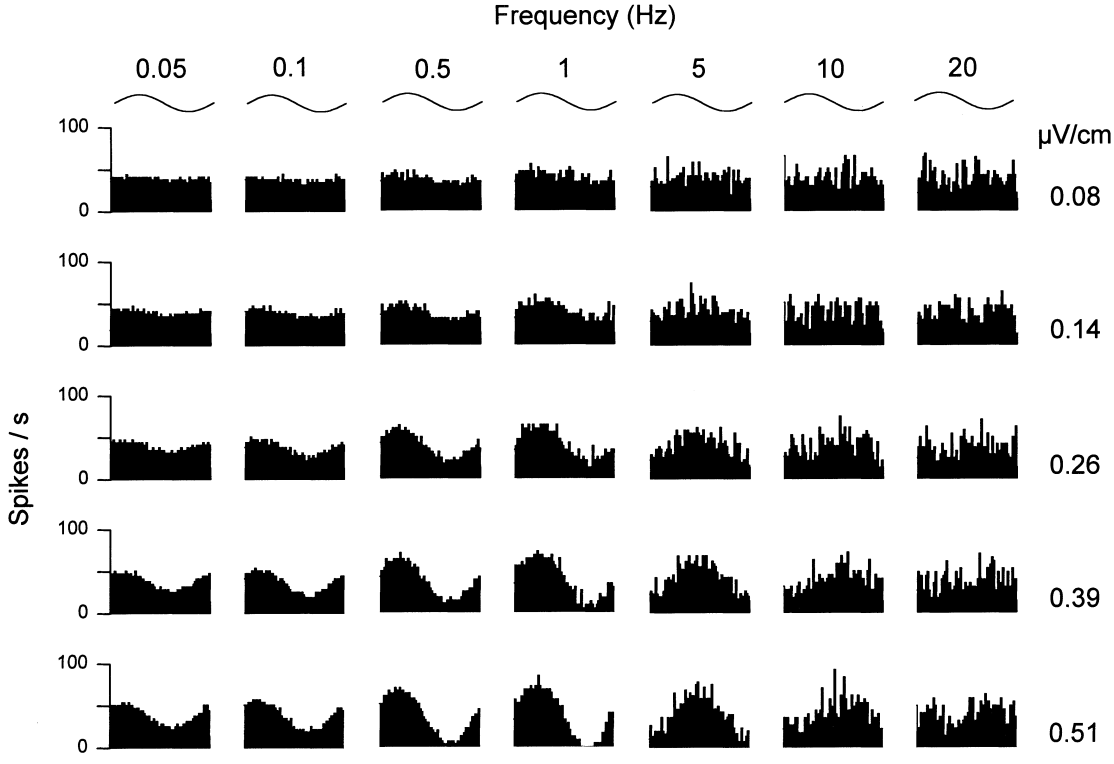

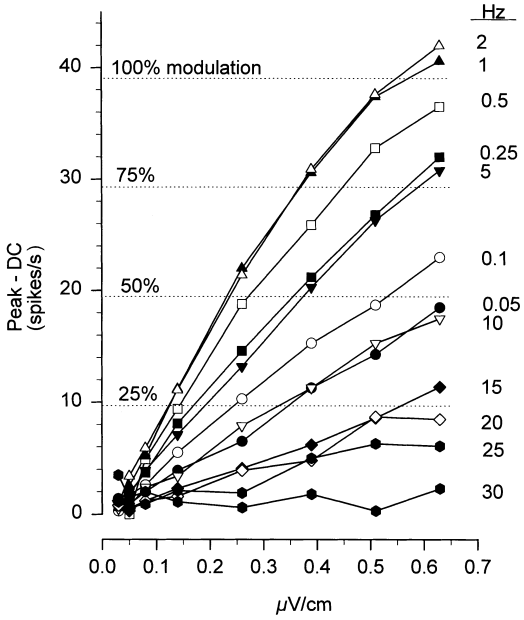

Fig. 8 Stimulus response of an electrosensory primary afferent across stimulus frequencies. Note greatest slope (sensitivity) is seen at frequencies of 1–2 Hz. Also note that curves above 50–75% modulation flatten. Stimulus intensity on abscissa is peak-to-peak

empirical peak (paired t-test, $df = 7$, $t = 10.9$, $P < 0.001$), and also the immediate post-peak rate of decline as shown for the unit in Fig. 9. Estimated time-constants from the exponential model for eight fibers ranged from 33.3 to 2.5 s with a mean of 8.3 s, and correspond to a low-pass cut-off from 0.005 to 0.064 Hz with a mean of 0.037 Hz.

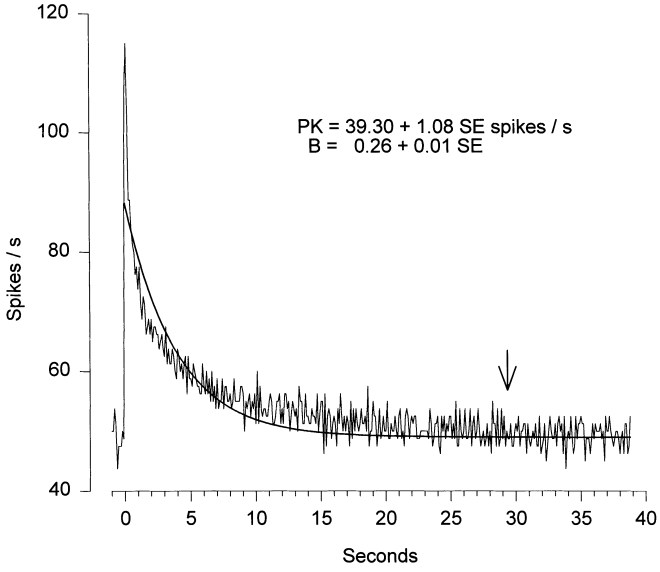

Fig. 9 Response of electrosensory primary afferent to stepped uniform d.c. field. Data are represented as average discharge across five consecutive d.c. steps (2.2 μV cm^{-1}) of 60 s duration. Best fit of negative exponential curve estimated a decay rate ($\beta = 0.26$) which translates to a time-constant of 4 s. *Arrow* indicates time when unit discharge returned to pre-stimulation resting rate

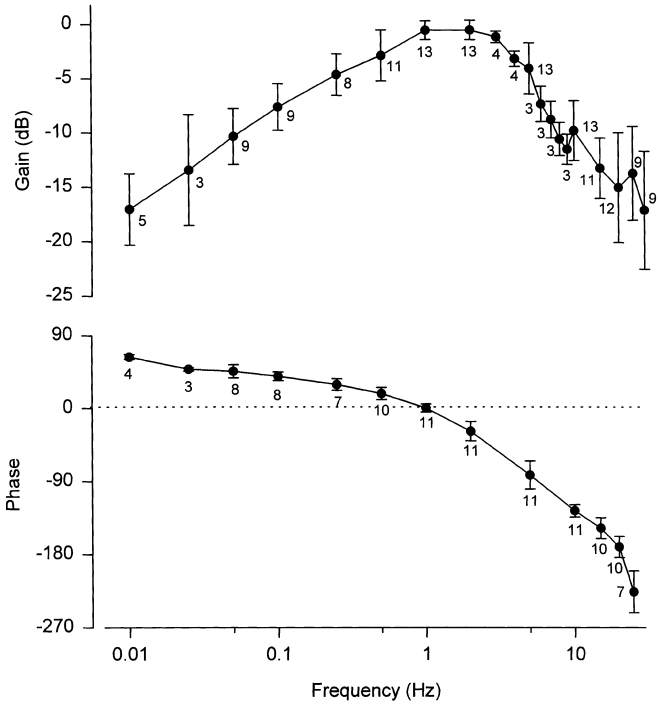

Fig. 10 Bode and phase plots for response of electrosensory primary afferent neurons. Units show best sensitivity at approximately 1–2 Hz stimulation with a 3-dB drop at about 0.5 Hz and 4 Hz. In order to control for different absolute sensitivity, data were calculated relative to peak response for each unit and expressed as relative dB. Phase plot shows peak neural response is in phase with stimulus at 1 Hz. Sample sizes indicated by numbers associated with each stimulus frequency in phase and Bode plot diagrams. *Vertical bars* indicate standard deviations

Linear frequency response analysis shows a homogeneous frequency sensitivity among electrosensory primary afferents. The frequency response to sinusoidal stimuli is summarized in the Bode plot and phase diagram shown in Fig. 10. Peak sensitivity for almost all units was at 1 or 2 Hz. The low variability of the 1- to 2-Hz peak frequency response and phase alignment at 1 Hz indicate homogeneity of the frequency responses among different electrosensory afferent fibers, and therefore also hyoid and mandibular canals of different lengths. Peak neural response to lower stimulus frequencies shows a gradual increase with a positive slope of 8.2 ± 0.3 dB/decade (mean ± SE). The low-frequency phase relationship for primary afferents shows a consistent phase lead near 45° with a frequency cross-over also at 1 Hz. At higher stimulus frequencies neural sensitivity rapidly decreased with a slope of −22.8 ± 0.4 dB/decade (mean ± SD) between 3 and 9 Hz. Above 1 Hz the response lag increases with frequency and phase is reversed at approximately 20 Hz.

Discussion

The results of this study add considerable new quantitative data about the sensitivity, dynamic range and

frequency-response characteristics of the elasmobranch electroreceptor system. Specifically, our study of *Urolophus* shows that primary afferents respond to weak bipolar voltage gradients as low as 20 ηV cm^{-1} peak, saturate over a wide range of field intensities, and that there is a non-linear relationship between unit response and near-threshold stimuli. Additionally, we demonstrate that the electrosensory system in *Urolophus* displays maximum sensitivity to stimulus frequencies near 1 Hz. Our discussion interprets these findings in relation to function of the electrosensory system in the ecology and natural behavior of elasmobranch fishes.

The DC of electrosensory primary afferents is an important determinant of the sensitivity and response properties of the elasmobranch electrosensory system. The average DC rate of 34 spikes s^{-1} at 18 °C for *Urolophus* is about two to three times that of the 18 spikes s^{-1} for *Platyrhinoidis* at 16–18 °C (Montgomery 1984b and the 11–14 spikes s^{-1} for *Raja* at 7 °C (New 1990; Montgomery and Bodznick 1993). One potential advantage for a rapid DC in the electrosensory system would be to enhance sensitivity by modulation of the discharge train and the elimination of a stimulus threshold necessary to evoke discharges (Aidley 1978). In a sensory system with spontaneously active primary afferents, any applied stimulus will affect the release of transmitter by the receptor cells, and subsequently affect the primary afferent discharge. Thus, stimulus detection then involves the central recognition of a change in primary afferent discharge pattern rather than the production of evoked spikes in a normally quiescent or slowly discharging system. In addition, an associated advantage for the relatively high DC rate as found in *Urolophus* would be an enhanced temporal resolution for encoding change in a varying stimulus.

Electrosensory primary afferent fibers that occur in the lateral line nerve of *Urolophus* and other batoid elasmobranchs form a relatively homogeneous population of regular discharging units (Andrianov et al. 1974, 1983; Akoev et al. 1976; Broun et al. 1979; Montgomery 1984b; New 1990; Montgomery and Bodznick 1993). This is in distinct contrast to the fish mechanosensory lateral line in which primary afferents exhibit multiple classes of DC patterns such as regular, irregular, burster, and silent (Munz 1985; Wubels et al. 1990; Tricas and Highstein 1991). One important theoretical advantage for the regular DC pattern found in all electrosensory primary afferents could be for optimal encoding of steady-state or low-frequency information as developed by Stein (1967) and applied to the vestibular system by Goldberg et al. (1984). In regular-type fibers, a change in electric field intensity would be encoded rapidly as a change in firing rate with a relatively high level of certainty because of the low endogenous variance in the resting interspike interval. The encoding of information is best when the stimulus frequency is much less than that of the unit's DC rate (Geisler 1968; Stein 1970). In *Urolophus*, the average resting rate (34 spikes s^{-1}) is an order of magnitude greater than the peak sensitivity of 1–2 Hz. In contrast, the encoding of low-frequency information by irregular-type units would have a relatively low certainty because of the high resting interspike interval variance. Primary afferents with irregular DCs better encode higher-frequency information as found in the fish lateral line and auditory systems which have peak frequency response decades above that of the elasmobranch electrosensory system (Coombs and Janssen 1989; Kroese and Schellart 1992; Schellart and Popper 1992). Thus, the regular DC pattern of primary afferent neurons may facilitate the high sensitivity to low-frequency electric stimuli.

The present experiments demonstrate modulation of the primary afferent discharges at peak intensities as low as 20 ηV cm^{-1}. Murray (1962) demonstrated a 1-μV cm^{-1} sensitivity to pulsed d.c. step stimuli in the short mandibular canals of the skate, while Andrianov et al. (1984) report neural responses in the skate to uniform sinusoidal fields as low as 30 ηV cm^{-1} PTP. Unfortunately, we did not attempt to routinely identify the canal length associated with each fiber because of the long time necessary to hold single units for intensity or frequency sweeps, and the risk of losing the unit by probing the body surfaces with a small dipole. This lack of information precludes calculation of a *relative* minimum stimulus level that might account for the effect of canal length which would be useful to compare responses among canals, clusters and species. It remains to be demonstrated whether the thresholds of primary afferents to weak fields are strictly a function of canal length, or perhaps also involve other morphological variables such as ampulla size, receptor number or receptor-to-primary afferent ratio.

Our measurements of the sensitivity of electrosensory primary afferents in *Urolophus* ($\bar{x} = 24$ spikes s^{-1} μV^{-1} cm^{-1}) are the highest yet reported by a single unit study in an elasmobranch. Electrosensory primary afferents in the thornback ray, *Platyrhinoidis*, show an approximately linear sensitivity of about 4 spikes s^{-1} μV^{-1} cm^{-1} when stimulated by much stronger uniform fields of 2–25 μV cm^{-1} (Montgomery 1984b). In the little skate, *Raja erinacea*, the sensitivity of primary afferents to a local dipole stimulus is 0.91 spikes s^{-1} μV^{-1} cm^{-1} (Montgomery and Bodznick 1993). The relatively high sensitivity found in this study for *Urolophus* is at least partially due to the use of a period histogram analysis which averages the response of many spikes over multiple stimulus cycles, and also our use of extremely weak fields to partially (as opposed to fully) modulate the resting discharge. This is best seen for high-gain units which exhibit a clear decline in the slope of the intensity-response relationship when the stimulus field gradient is increased from a few tens to a few hundreds of ηV cm^{-1} (Fig. 6). Thus, one important conclusion of this study is that the response features of the ampullary electrosensory system in the elasmobranch appear to be intensity dependent, and that the electrosensory system is most sensitive to near-threshold electric fields. The exquisite sensitivity at near-threshold intensities is especially

relevant when one considers the adaptive value of detecting prey (Kalmijn 1971; Tricas 1982) or mates (Tricas et al. 1995) at distance, or the possible use of weak electric fields for directional information (Kalmijn 1974; Paulin 1995).

The sensitivity of primary afferents in *Urolophus* is more like that of second-order electrosensory neurons, also known as principal cells or ascending efferent neurons (AENs), recorded in the medulla of the thornback ray, *Platyrhinoidis*. AENs in the thornback exhibit a sensitivity of about 32 spikes s^{-1} μV^{-1} cm^{-1} and depart from linearity at stimulus levels < 1 μV cm^{-1} (Montgomery 1984b). Although we have yet to empirically determine the intensity-response function for AENs in *Urolophus*, there is evidence to suggest that they should be even more sensitive than electrosensory primary afferents. The sensory epithelium of each surface pore-ampulla complex consists of hundreds of receptor cells which receive a common stimulus that is identical both in amplitude and phase. Each hyoid ampulla is innervated by approximately ten primary afferent neurons (T.C. Tricas and M. Sandrene, unpublished observations) and therefore there is a high degree of convergence of individual receptors onto each primary afferent. A consequence of this convergence is the averaging of postsynaptic noise caused by the random release of transmitter from a large number of receptor cells. This results in an increase in the postsynaptic signal-to-noise ratio and an enhanced neural sensitivity as discussed for the electric teleost ampullary system by Zakon (1987). We suggest that parallel primary afferent channels from a common ampulla will also reduce postsynaptic noise at the level of the AEN. The regular resting spontaneous activity of each primary afferent produces an unsynchronized release of excitatory transmitter onto the principal cell. If the total primary afferent population ($n = 10$) for each ampulla projects to a common AEN, the postsynaptic signal-to-noise ratio at the principal cell level would also increase by a factor of $\sqrt{n}$, or about threefold compared to that for a single primary afferent channel. This could enhance detection of a stimulus-induced change in primary afferent DC, which unlike that of synaptic noise is synchronized among all afferents of a single ampulla. Applying this simple estimate of signal-to-noise enhancement to our lowest measured stimulus intensity (20 ηV $cm^{-1}/\sqrt{10}$), the sensitivity of the AEN should be near or possibly even lower than the 5 ηV cm^{-1} behavioral threshold reported for this species by Kalmijn (1982). AENs are known to receive excitatory input from one to several adjacent skin pores (review: Montgomery et al. 1995); thus, at least in the former case there should exist a complete projection of the primary afferents from one ampulla to a single principal cell. However, AENs that have a receptive field which includes several pores must also show convergence of primary afferents from different ampullae. It is currently unknown what degree of excitatory fidelity exists between each ampulla and the population of AENs, such as possible primary afferent axon collaterals that project to multiple AENs or the projection of each primary afferent to a single AEN. While it is possible that convergence of primary afferents from different ampullae upon a single AEN could ultimately increase the magnitude of the encoded signal, further neuroanatomical and physiological studies are needed to model the circuitry.

The neural response of electrosensory primary afferents in *Urolophus* demonstrates at least a 40-fold range of sensitivities among units, and also that the rate-intensity response is lost as the unit approaches full modulation. The wide range of observed neural sensitivities and saturation levels is at least partly a function of the ampulla canal length which in adult *Urolophus* varies from about 1 mm in the mandibular cluster to >10 cm in the hyoid cluster. We suggest this > 100-fold range of canal lengths in a single animal serves an important biological function. Ampullae of Lorenzini act as core conductors in which the internal lumen of the receptor is isopotential with the opening of the canal pore in the epidermis (Obara and Bennett 1972). Each low-resistance canal terminates in a bulbous ampulla in which the apical membranes of the electroreceptor cells are joined by tight junctions. The receptor potential is a function of the voltage drop across the receptor's apical (isopotential with the associated skin pore) and basal (isopotential with the internal tissues of the animal) surfaces. Thus, in a uniform field parallel to the canal, the maximum receptor potential and associated primary afferent sensitivity are constrained by the length of the associated canal. In batoids, the longest ampullary canals are distributed around the periphery of the pectoral disk while most shorter canals are distributed around the snout, head, and mouth. This morphological organization supports the hypothesis that batoids such as *Urolophus* use the long, highly sensitive canals for the detection of (and orientation to) weak fields produced by visually cryptic prey (Kalmijn 1971; Tricas 1982), conspecifics (Tricas et al. 1995), or possibly those of geomagnetic origin (Murray 1962; Kalmijn 1974, Paulin 1995). Primary afferent neurons associated with short canals have a lower sensitivity, a wider dynamic response range and require a higher intensity for discharge saturation. In contrast, these features would be advantageous for localizing the source at close range when the field is relatively intense such as during final approach to a mate or positioning of the mouth over the prey.

The frequency response of electrosensory primary afferents demonstrates a peak sensitivity at 1–2 Hz and a rapid high-frequency roll-off. This peak sensitivity in *Urolophus* is distinctly lower than the 5–7 Hz for the thornback ray, *Platyrhinoidis* (Montgomery 1984b) and narrower than 1–5 Hz reported for the little skate, *Raja* (New 1990). In contrast, peak frequency sensitivities are higher than the 0.1–0.5 Hz reported for Black Sea batoids, *Trygon pastinaca* and *Raja clavata* (Andrianov et al. 1984). The frequency of peak sensitivity for electrosensory afferents in *Urolophus* is most similar to the best frequency of the electrically evoked respiratory

reflex (0.5–1.0 Hz) reported in the cat shark, *Scyliorhinus canicula*, but is well below the 5–10 Hz peak neural sensitivity recorded from electrosensory primary afferents (Peters and Evers 1985). The peak sensitivity at low frequency of elasmobranch electroreceptor systems must function to enhance detection of numerous forms of biologically important phasic stimuli that are encountered by elasmobranch fishes in the wild. All aquatic prey produce a standing d.c. field that appears to vary at low frequency as the elasmobranch receptor system passes through it (Kalmijn 1988) or alternatively as the prey moves relative to a resting elasmobranch predator. In addition, d.c. fields produced by prey fishes are modulated during ventilatory movements of the mouth and operculi (Kalmijn 1974) often near 1–2 Hz but remain to be demonstrated as an important phasic signal in prey detection. Recent investigations of a wild population of *Urolophus* show that male stingrays use electroreception to locate visually cryptic females concealed in the sand substrate from distances up to about 1 m (Tricas et al. 1995). Like other fishes, the stingrays also produce a significant standing field that is partially modulated by ventilatory activity. The 1-Hz spectrum peak of the field modulation produced by the animal's ventilatory activity matches the peak sensitivity of the electrosensory afferents. This phasic signal may be important for the detection of conspecific individuals during active swimming, and especially when rays are aggregated at rest on the bottom. Since *Urolophus* electrosensory afferents adapt to d.c. stimuli such as a standing field within seconds, only the modulated portion of the bioelectric field will be detectable when animals are at rest on the bottom and near to each other.

In addition to the production of standing field potentials, many elasmobranchs also posses active discharge organs that produce a train of pulsed electric organ discharges (EODs). Skates of the family Rajidae routinely discharge their weak electrogenic organs when engaged in social interactions (Bratton and Ayers 1987). Although EODs remain to be demonstrated as important for social communication, there is evidence for electrosensory tuning of natural EOD stimuli. For example, the peak frequency sensitivity of electrosensory afferents in *R. erinacea* is near the 5-Hz principal spectral component of the skate's EOD (New 1990, 1994). Furthermore, in adult clear noseskates, *Raja eglanteria*, the average EOD pulse rate is aligned with peak tuning (J. Sisneros and T.C. Tricas, unpublished observations). Thus, the electrosensory systems of electrogenic elasmobranchs may experience selective pressure to encode both the slowly varying fields discussed above, and also the pulsed electric field stimuli used in social communication.

A recent theoretical model suggests that low-frequency periodic movements of sharks swimming through the horizontal component of the earth's magnetic field can induce periodic vertical electric fields through the head and body that may be integrated with vestibular information and used for geonavigation behavior (Paulin 1995). The detection of a change in an extremely weak periodic field could theoretically be detected centrally by averaging neural responses over many cycles of head rotation, which for most sharks occurs at frequencies near 1 Hz (T.C. Tricas, unpublished observations). In this study we demonstrate maximum sensitivity to a 20-ηV cm^{-1} uniform field at 1 Hz by averaging the response of only 500 spikes over a period of about 10–15 s. Thus, it seems reasonable to assume that the central processing of electric stimuli by the elasmobranch brain should also be optimized to detect small changes in these induced periodic stimuli. Future work should continue to evaluate the comparative physiology and anatomy of the elasmobranch electrosensory processing system in relation to the evolution of its natural behavioral functions and ecology.

Acknowledgements This work was supported by a grant from the Whitehall Foundation to T.C.T. and NIH (NS30194) to J.G.N. We thank F. Wang, E. Coots, C. Inman, D. Bodznick, M. Sandrene, S. Highstein, M. Thursby, Cambridge Electronics Design and Carl Zeiss, Inc. for technical support; and S. Highstein, M. Paulin, J. Montgomery, J. B. Sisneros, H. Zakon and especially two anonymous reviewers for comments that greatly improved the manuscript. Experimental procedures followed NIH guidelines for the care and use of animals and were approved by the Institutional Animal Care and Use Committee at Florida Institute of Technology.

References

Aidley DJ (1978) The physiology of excitable cells. Cambridge University Press, Cambridge

Akoev GN, Ilyinsky OB, Zadan PM (1976) Physiological properties of electroreceptors of marine skates. Comp Biochem Physiol 53A: 201–209

Andrianov GN, Broun GR, Ilyinsky OB (1974) Responses of central neurons to electrical and magnetic stimuli of the ampullae of Lorenzini in the Black Sea skate. J Comp Physiol 93: 287–299

Andrianov GN, Broun GR, Ilyinsky OB (1983) Electrophysiological study of central projections of ampullae of Lorenzini in skates, *Raja radiata*. Neurophysiology 15: 451–457

Andrianov GN, Broun GR, Ilyinsky OB (1984) Frequency characteristics of skate electroreceptive central neurons responding to electrical and magnetic stimulation. Neurophysiology 16: 365–376

Bodznick DA, Boord RL (1986) Electroreception in Chondrichthyes: central anatomy and physiology. In: Bullock TH, Heiligenberg W (eds) Electroreception. Wiley, New York, pp 225–256

Bodznick DA, Montgomery JC, Bradley DJ (1992) Suppression of common mode signals within the electrosensory system of the little skate, *Raja erinacea*. J Exp Biol 171: 107–125

Bodznick DA, Hjelmstad G, Bennett MVL (1993) Accommodation to maintained stimuli in the ampullae of Lorenzini: how an electroreceptive fish achieves sensitivity in a noisy world. Jpn J Physiol 43. [Suppl 1]: S231–S237

Bratton BO, Ayers JL (1987) Observations on the electric organ discharge of two skate species (Chondrichthyes: Rajidae) and its relationship to behaviour. Environ Biol Fish 20: 241–254

Braun HA, Wissing H, Schafer K, Hirsch MC (1994) Oscillation and noise determine signal transduction in shark multimodal sensory cells. Nature 367: 270–273

Broun GR, Ilyinsky OB, Krylov BV (1979) Responses of the ampullae of Lorenzini in a uniform electric field. Neurophysiology 11: 158–166

Coombs S, Janssen, J (1989) Peripheral processing by the lateral line system of the mottled sculpin (*Cottus bairdi*). In: Coombs S, Gorner P, Munz H (eds) The mechanosensory lateral line. Springer, Berlin Heidelberg, New York, pp 299–319

Dijkgraaf S, Kalmijn AJ (1966) Versuche zur biologischen Bedeutung der Lorenzinischen Ampullen bei den Elasmobranchiern. Z Vergl Physiol 53: 187–194

Geisler CD (1968) A model of the peripheral auditory system responding to low-frequency tones. Biophys J 8: 1–15

Goldberg JM, Smith CE, Fernandez C (1984) Relation between discharge regularity and responses to externally applied galvanic currents in vestibular nerve afferents of the squirrel monkey. J Neurophysiol 51: 1236–1256

Kalmijn AJ (1971) The electric sense of sharks and rays. J Exp Biol 55: 371–383

Kalmijn AJ (1974) The detection of electric fields from inanimate and animate sources other than electric organs. In: Fessard A (ed) Handbook of sensory physiology, vol III/3. Springer, Berlin Heidelberg New York, pp 147–200

Kalmijn AJ (1982) Electric and magnetic field detection in elasmobranch fishes. Science 218: 915–918

Kalmijn AJ (1988) Detection of weak electric fields. In: Atema J, Fay RR, Popper AN, Tavolga WN (eds) Sensory biology of aquatic animals. Springer, Berlin Heidelberg New York, pp 151–186

Kroese ABA, Schellart NAM (1992) Velocity- and acceleration-sensitive units in the trunk lateral line of the trout. J Neurophysiol 68: 2212–2221

Montgomery JC (1984a) Noise cancellation in the electrosensory system of the thornback ray; common mode refection of input produced by the animal's own ventilatory movement. J Comp Physiol A 155: 103–111

Montgomery JC (1984b) Frequency response characteristics of primary and secondary neurons in the electrosensory system of the thornback ray. Comp Biochem Physiol 79 A: 189–195

Montgomery JC, Bodznick D (1993) Hindbrain circuitry mediating common-mode suppression of ventilatory reafference in the electrosensory system of the little skate, *Raja erinacea*. J Exp Biol 183: 203–215

Montgomery JC, Coombs S, Conley RA, Bodznick D (1995) Hindbrain sensory processing in lateral line, electrosensory, and auditory systems: a comparative overview of anatomical and functional similarities. Aud Neurosci 1: 207–231

Munz H (1985) Single unit activity in the peripheral lateral line system of the cichlid fish *Sarotherodon niloticus* L. J Comp Physiol A 157: 555–568

Murray RW (1962) The response of the ampullae of Lorenzini of elasmobranchs to electrical stimulation. J Exp Biol 39: 119–128

Murray RW (1965) Electroreceptor mechanisms: the relation of impulse frequency to stimulus strength and responses to pulsed stimuli in the ampullae of Lorenzini of elasmobranchs. J Physiol (Lond) 180: 592–606

New JG (1990) Medullary electrosensory processing in the little skate. I. Response characteristics of neurons in the dorsal octavolateralis nucleus. J Comp Physiol A 167: 285–294

New JG (1994) Electric organ discharge and electrosensory reafference in skates. Biol Bull 187: 1–12

Obara S, Bennett MVL (1972) Mode of operation of ampullae of Lorenzini of the skate, *Raja*. J Gen Physiol 60: 534–557

Paulin MG (1995) Electroreception and the compass sense of sharks. J Theor Biol 174: 325–339

Peters RC, Evers HP (1985) Frequency selectivity in the ampullary system on an elasmobranch fish (*Scyliorhinus canicula*). J Exp Biol 118: 99–109

Schellart NAM, Popper AN (1992) Functional aspects of the evolution of the auditory system of actinopterygian fish. In: Webster DB, Fay RR, Popper AN (eds) The evolutionary biology of hearing. Springer, Berlin Heidelberg New York, pp 295–322

Sokal RR, Rohlf FJ (1981) Biometry. Freeman, New York

Stein RB (1967) The information capacity of nerve cells using a frequency code. Biophys J 7: 797–826

Stein RB (1970) The role of spike trains in transmitting and distorting sensory signals. In: Schmitt FO (ed) The neurosciences – second study program. Rockefeller University Press, New York, pp 597–604

Tricas TC (1982) Bioelectric-mediated predation by swell sharks, *Cephaloscyllium ventriosum*. Copeia 1982: 948–952

Tricas TC, Highstein S (1991) Visually mediated inhibition of lateral line primary afferent activity by the octavolateralis efferent system during predation in the free-swimming toadfish, *Opsanus tau*. Exp Brain Res 83: 233–236

Tricas TC, Michael SW, Sisneros JA (1995) Electrosensory optimization to conspecific phasic signals for mating. Neurosci Lett 202: 129–132

Wubbels RJ, Kroese ABA, Duifhuis H (1990) Afferent bursting activity of ruff lateral line induced by background noise stimulation. J Comp Physiol A 166: 585–588

Zakon HH (1987) Variation in the mode of receptor cell addition in the electrosensory system of gymnotiform fish. J Comp Neurol 262: 195–214